Geomorphology 454 (2024) 109150

Contents lists available at ScienceDirect

Geomorphology

journal homepage: www.journals.elsevier.com/geomorphology

Exploring nearshore bed dynamics of a mixed beach using the depth of closure conceptual model

Dominique Townsend [a,*], Julian Leyland [a], Hachem Kassem [b], Charlie Thompson [b,c], Ian Townend [b]

[a] School of Geography and Environmental Science, University Road, Southampton, Hampshire SO17 1BJ, UK
[b] School of Ocean and Earth Science, University of Southampton, Waterfront Campus, National Oceanography Centre, European Way, Southampton, SO14 3ZH, UK
[c] Channel Coastal Observatory, Waterfront Campus, National Oceanography Centre, European Way, Southampton, SO14 3ZH, UK

ARTICLE INFO

Keywords:
Depth of closure
Nearshore morphology
Mixed beaches
Coastal steepening

ABSTRACT

Mixed sediment beaches are globally commonplace, yet little is understood of the extent and behaviour of their nearshore zones, potentially underestimating total cross-shore change. This paper is the first study to investigate the lateral and vertical extent of the active zone of the gravel-rich mixed beach in Pevensey Bay, a study site on the South East UK coastline. Morphodynamic change in the nearshore zone was studied at a range of timescales (days, months, years) suggesting that the width of the active nearshore zone correlated with the magnitude of the peak morphological change, whilst the depth of closure was influenced by bed slope, grain size and local variation in wave conditions. A conceptual model detailing the physical parameters responsible for local variations in the depth of closure was used to help understand differences between the observed and predicted depths of closure. Finally, ongoing chronic loss of sediment from below Mean Sea Level (MSL) was examined, which was shown to be independent of the depth of closure, but closely linked to the wider geomorphic setting of the bay.

1. Introduction

The nearshore zone (defined here as the area extending from the highest reach of the swash zone to the point at which waves begin to shoal) is a complex and dynamic environment that plays a critical role in coastal processes, ecological systems, and related human activities. Understanding its dynamics and morphology is important for effective coastal management and for maintaining the health and resilience of coastal communities and ecosystems. Bedforms and shoreline morphology combine to dissipate or focus wave energy, in turn influencing sediment transport and erosional and depositional dynamics. These process-form interactions are further complicated by the nature of the sediment found in the nearshore zone, specifically in terms of grain size distribution and spatial variability.

When considering the extent of the nearshore, a useful theoretical concept is that of the depth of closure, which marks the seaward extent of the nearshore zone, as the point at which the seabed becomes morphologically inactive over a specified timescale (Kraus et al., 1998). The concept was originally devised to pinpoint a limit to seasonal bed movements in sandy beaches to assist in beach nourishment design (Hallermeier, 1977, 1978, 1981). However, the depth of closure is now widely applied in engineering design, providing boundaries to both sediment budgets and coastal modelling tools (de Figueiredo et al., 2020) for a wide range of open-coast environments (Brutsché et al., 2015). Broadly, the literature on the depth of closure addresses field methods and predictive models. The former includes methods to identify the point of closure through repeat bathymetric surveys (*e.g.* Birkemeier, 1985; Nicholls et al., 1998a; Hartman and Kennedy, 2016), analysis of sediment facies (*e.g.* Dumas and Arnott, 2006), or grain size analysis (*e.g.* Aragonés et al., 2018). On the other hand, predictive methods for estimating the depth of closure include: equations accounting for wave parameters only (*e.g.* Hallermeier, 1978; Birkemeier, 1985; Nicholls et al., 1998a), utilising equilibrium profile theory (*e.g.* Nicholls et al., 1998b; Ortiz and Ashton, 2016), as well as including data on sediment size and incident wave angle utilising machine learning approaches (*e.g.* Aragonés et al., 2015). A number of studies seek to improve understanding of the depth of closure through the comparison between the predicted and the observed closure depth (Hinton and Nicholls, 1998; Robertson et al., 2008; Polska et al., 2015; Hartman and Kennedy, 2016; Valiente et al., 2017; Aragonés et al., 2019; Udo et al., 2020; Barrineau

* Corresponding author.
E-mail address: D.Townsend@soton.ac.uk (D. Townsend).

https://doi.org/10.1016/j.geomorph.2024.109150
Received 4 August 2023; Received in revised form 8 March 2024; Accepted 9 March 2024
Available online 13 March 2024

et al., 2021). A conceptual summary of the physical parameters influencing the depth of closure is provided in Fig. 1 and can be used to help interpret local variations in the depth of closure obtained from repeat bathymetry data. There are three main components which can moderate the depth of closure, namely waves and currents, bed morphology/slope and sediment composition:

• Waves and currents: The presence and magnitude of waves directly impact the energy available to entrain sediment in the nearshore and therefore as a coastline becomes more exposed, the energy available to mobilise material increases (Nicholls et al., 1996; Francois et al., 2005). Similarly, as the incident wave angle approaches 45°, the maximum wave radiation stresses are reached and maximum transport occurs (Ashton and Murray, 2006). Currents have also been shown to moderate the depth of closure by suppressing or enhancing bed level change (Kraus et al., 1998; Valiente et al., 2019).

• Bed morphology: Bed morphology can vary greatly depending on underlying geology and the availability of superficial sediments (Robertson et al., 2008; Hartman and Kennedy, 2016; Anthony and Aagaard, 2020). A key factor on how the morphology affects the depth of closure is the bed slope, as a greater slope allows for greater offshore transport (downslope) (Ortiz and Ashton, 2016; Hamon-Kerivel et al., 2020).

• Sediment composition: The critical threshold for sediment entrainment is related to grain size and therefore this is an important factor in determining the depth of closure (Udo et al., 2020). In mixed sediment environments, the presence of gravel and/or mud can increase the amount of energy required to mobilise sand (Panagiotopoulos et al., 1994; Mitchener and Torfs, 1995; McCarron et al., 2019). Sediment properties, the presence of biota (biofilms to macroalgae) and natural cementation also alter the critical bed shear stress needed for entrainment.

This conceptual model can be used to help interpret local and regional variation in the depth of closure, where the observed depth of closure is different to that estimated by established empirical formulae (*cf.* 2.1 Depth of closure – wave energy approach).

Beach management activities, including beach recharge, recycling

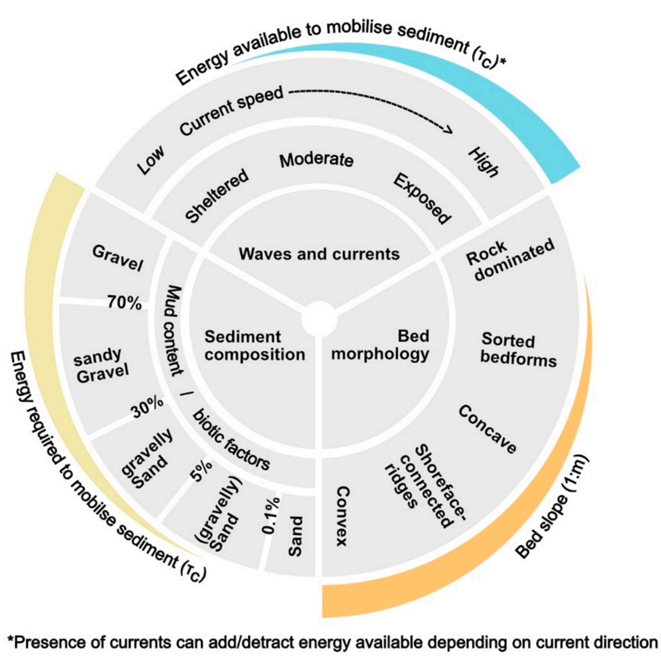

Fig. 1. The physical parameters influencing the depth of closure; waves and currents, bed slope, and sediment composition are shown in relation to the influences on depth of closure, namely, 'Energy required to mobilise sediment' (yellow), 'Energy available to mobilise sediment' (blue), and 'Bed slope' (orange). (For interpretation of the references to colour in this figure legend, the reader is referred to the web version of this article.)

and bypassing, have been employed globally to counter erosion along highly-populated coasts (de Schipper et al., 2021; Staudt et al., 2021). With limited effects on downdrift sediment supply, these 'soft' engineering approaches have been adopted widely despite requiring higher levels of intervention than traditional 'hard' engineering. In recent years, the social, ecological and geomorphological sustainability of these schemes have been brought into question (Parkinson and Ogurcak, 2018; Staudt et al., 2021) although much of the focus has been on sandy shores. For decades, soft engineering works have been carried out on mixed sediment beaches on the south eastern English coastline with little consideration of the nearshore zone as the predominantly gravel upper beach is often treated as a fixed coastal defence, independent from its surroundings (Dornbusch and Hardiman, 2020). Our study site, Pevensey Bay, East Sussex, UK, is a key example of this, and concerns have been raised over the long term sustainability of the current management approach, as over a thirteen year period approximately 8000 m^3 of sediment from below the mean sea level mark have been lost from the 9 km long frontage each year (Thomas, 2015). This paper examines the relationship between the shoreline management of the upper beach and the nearshore zone, by measuring width and depth of the nearshore zone in a mixed sediment environment over time, using the depth of closure concept. Bathymetric data covering short (days) to medium (months to years) timescales for the mixed sediment beach of Pevensey Bay are used to address the following objectives:

1) compare observed and predicted depths of closure for a mixed sediment environment;

2) interpret temporal and spatial differences in the observed depth of closure using the conceptual model set out in Fig. 1; and.

3) understand the changes in the nearshore zone in relation to the current shoreline management.

1.1. Study site

The study site, Pevensey Bay, is a 9 km barrier beach located on the East Sussex coast, southeast England, UK (Fig. 2). The beach at Pevensey is described as a composite mixed beach, comprising a reflective, mixed sand gravel upper beach and a dissipative sandy foreshore/low-tide terrace (Horn and Walton, 2007; Sutherland and Thomas, 2011). The upper mixed sand gravel beach has a median grain diameter (D_{50}) ranging between 8 and 16 mm across the site (Watt et al., 2006). Six trial pits dug at the high water mark down to 0 mOD revealed an upper predominantly gravel layer (less than 5 % sand), approximately 0.1 m deep capping the beach sediments, and a higher sand content below this layer between 10 and 40 % sand, which resulted in a median diameter (D_{50}) ranging between *c.* 3 mm to just over 30 mm as the percentage of sand varied with depth (Dornbusch et al., 2005a,Dornbusch et al., 2005b). Visual interpretation of multibeam backscatter data, whereby surface roughness can be inferred, suggested a largely sandy bed with outcrops of gravel in the centre of the site, with an area of mixed sediment in the west and exposed rock outcrops to the eastern extent within a kilometre of the coastline (Channel Coastal Observatory, 2014).

The bay is mostly exposed to large south westerly waves (Hs $\leq$2.5 m) for ~85 % of the time, and smaller, less frequent easterly waves (Hs $\leq$1.5 m) for ~15 % of time (Fig. 2, Sutherland and Thomas, 2011). Wave conditions are typically calm in the summer period between April and August (Hs ~0.6 m), and are more energetic in the winter period between September and March, with average monthly Hs peaking at just over 1.0 m in December (National Network of Regional Coastal Monitoring Programmes., n.d.). The spring and neap tidal ranges are 6.7 m and 2.3 m respectively (Horn and Walton, 2007; Elsner et al., 2015). Depth averaged tidal currents vary from an average rate of 0.5 ms^{-1} at mean spring conditions to 0.3 ms^{-1} during mean neap conditions, and residual (non-tidal) currents have been shown to flow as quickly as 0.71 ms^{-1}, with average flows generally between 0.11 and 0.04 ms^{-1} (Fugro Emu Ltd., 2016). The beach is actively managed as a flood asset, protecting approximately 50 km^2 of low-lying land, *c.*10,000 properties as

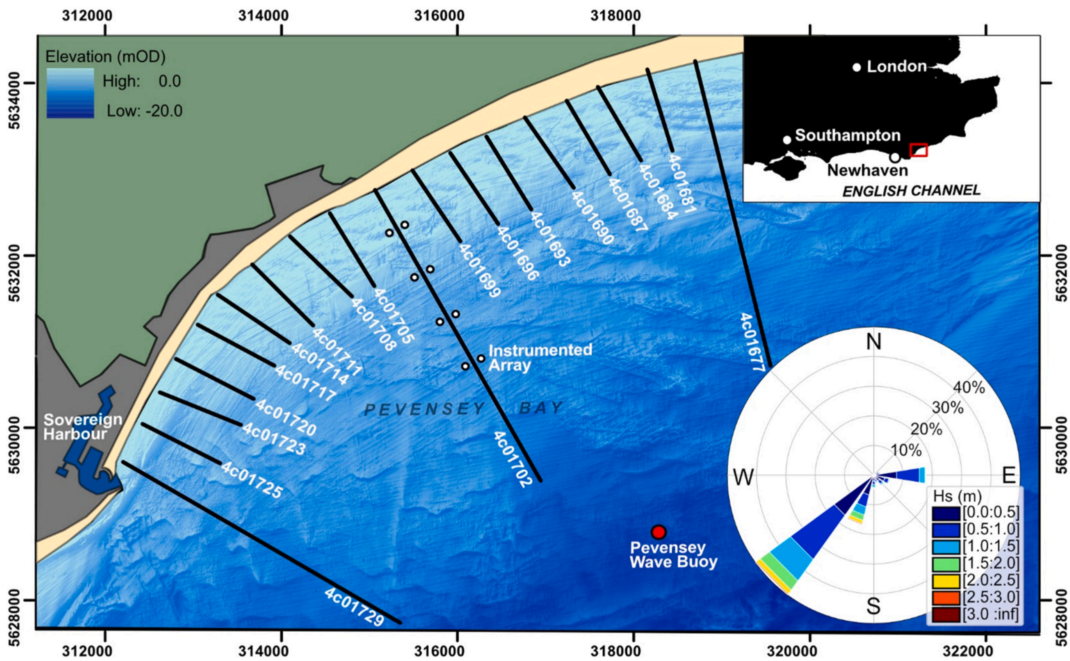

Fig. 2. Pevensey Bay study site; green and grey areas showing rural and urban land use, respectively. Yellow area representing upper beach. Black profile lines show the position of bathymetric surveys with names corresponding to the National Network of Regional Coastal Monitoring Programme (NNRCMP) beach profiles. The wave rose shows binned data from the Pevensey Wave buoy (position shown by red marker) for the period June 2003 – November 2022. Bathymetric data composite of 2012 Centre for Environmental Fisheries and Aquaculture Science (CEFAS), 2013 Channel Coastal Observatory (CCO) data (1 km inshore) and 2015 Maritime and Coastguard Agency (MCA). Inset map showing the south east of England and the regional setting of Pevensey Bay. Grid projection: UTM 31 N. (For interpretation of the references to colour in this figure legend, the reader is referred to the web version of this article.)

well as nationally and internationally important wildlife sites from inundation (Sutherland and Thomas, 2011). To maintain the barrier width and beach volume, each year an average of 80,000 m^3 of sediment are recycled within the study site, 10,000 m^3 are bypassed into the site from west of the Sovereign Harbour breakwaters and a further 20,000 m^3 are recharged from an offshore source, Owers Bank, 9 km offshore of Littlehampton, West Sussex and ~ 60 km west of the study site (Thomas 2023, pers. comm.).

2. Methods

The following section details five stages of work. Firstly, the estimation of depth of closure from hydrodynamic input is given (2.1 Depth of closure – wave energy approach), followed by the identification of the observational depth of closure including description on the collection and interpretation of 19 years of bathymetry data with variable temporal resolution within that period (2.2 Depth of closure – observational approach). Long and cross-shore sediment transport are also estimated at three inshore locations (2.3 Nearshore transport estimation). The method for sediment grain size analysis is documented (2.4 Sediment analysis). Finally, a sediment balance exercise is described comprising an analysis of the upper beach slope over time and cross sectional area of the nearshore (2.5 Sediment balance).

2.1. Depth of closure – Wave energy approach

The seasonal limit to sand movement, also referred to as the inner limit (d_l), was calculated using the Hallermeier (1977, 1978) and Birkemeier (1985) eqs. (1)–(4) for comparison to depth of closure measurements from observational data. The equation for the inner limit as given by Hallermeier (1978) is:

$$d_{lh} = 2.28H_e - 68.5\left(\frac{H_e^2}{gT_e^2}\right) \tag{1}$$

where g is the acceleration due to gravity, H_e is the non-breaking significant wave height exceeded 12 h per year, and T_e is the associated wave period. The 12 hourly exceedance was taken from the wave record between 08/07/2003 and 31/10/2019 of the Pevensey Bay Wave Buoy, which is recording in a water depth of approximately 9.8 m below Chart Datum (Fig. 2) and is available to freely download from the Channel Coastal Observatory website at https://coastalmonitoring.org/.

Hallermeier (1977) simplified equation for the inner limit is:

$$d_{lhs} = 2\overline{H}_s + 11\sigma_s \tag{2}$$

where $\overline{H}_s$ is the annual, mean significant wave height and σ_s is the associated standard deviation. Birkemeier (1985) adjusted the equation for the inner depth of closure:

$$d_{lb} = 1.75\ H_e - 57.9\left(\frac{H_e^2}{gT_e^2}\right) \tag{3}$$

and Birkemeier (1985) simplified the equation:

$$d_{lbs} = 1.57\ H_e \tag{4}$$

Whilst Hallermeier's d_l gives a 'seaward limit to extreme surf-related effects', they recognized that waves begin to interact with the seabed through shoaling, further offshore. To mark the start of the shoaling zone, Hallermeier identified the outer closure limit (d_i), using both mean annual wave values and the median grain size (D_{50}). This zone represents a 'buffer area where expected waves have neither strong nor negligible effects on the sand bed during a typical annual cycle of wave action' (Hallermeier, 1981). This is the deepest limit that wave-driven bed level change will occur. This was calculated herein using Hallermeier (1983) revised equation:

$$d_i = 0.018H_mT_m\sqrt{\frac{g}{D_{50}(s-1)}} \tag{5}$$

where H_m is the mean annual significant wave height, T_m is the associated wave period, D_{50} the median sediment size and s is the specific gravity (ratio of sediment density to water density). The D_{50} used herein was taken as the average grain size for sediments found on the foreshore from samples taken on the 19/11/2019 as detailed in 2.4 Sediment analysis.

2.2. Depth of closure – Observational approach

2.2.1. Data collection

A series of bathymetry surveys were undertaken at the study site, namely two 'bay wide' surveys, consisting of 18 shore normal profiles (aligned with existing National Network of Regional Coastal Monitoring Programmes for England (NNRCMP) beach profiles) on the 15/09/2020 and 30/03/2021 with an aim to capture change over the 2020/2021 winter storm season (September to March). The profiles extended 1 km offshore, with the exception of three profiles, 4c01677, 4c01702 and 4c01729 which extended out to the estimated Hallermeier's outer depth of closure, d_i, (eq. 5), between 3.6 and 3.9 km offshore (Fig. 2). For simplicity these extended profiles are referred to as the Easternmost (4c01677), Central (4c01702) and Westernmost (4c01729) profiles throughout the text. The extended profiles were also surveyed on the 14/04/2022, and Profile 4c01702 was surveyed (in part) an additional six times between March 2021 and February 2022, Table 1. For every bathymetric survey completed, a complimentary upper beach topographic survey was carried out during the preceding/subsequent low water periods to gain a full picture of the beach profile. This was done by the University of Southampton or by Adur-Worthing Councils, as part of the Southeast Regional Coastal Monitoring Programme. All topographic data crossed the highest sub-aerial elevation of the beach, but, beyond this point most data were limited by private property boundaries. Topographic data were collected using real time kinematic Global Navigation Satellite System (GNSS) equipment, whereby points were collected at a maximum of 5 m spacing across the beach profiles with additional points recorded if a change in slope was observed. This approach is consistent with the NNRCMP.

Bathymetric surveys were carried out by the University of Southampton and external IHO Category A contractors, the details of which are provided in the supplementary information. Single-Beam Echo Sounding (SBES) was used for the bay wide surveys, whilst Multi-Beam Echo Soundings (MBES) were used for all but one of the surveys of the Central profile 4c01702. The horizontal resolution varied between 0.01 and 0.5 m; the vertical resolution was sub-centimetre for all systems. The horizontal error ranged between ±0.03 m and ± 0.10 m, and the vertical error ranged between ±0.06 m and ± 0.3 m (New Forest District Council, 2020; Shoreline Surveys Ltd, 2021; Unmanned Survey Solutions, GeoSight, HydroSurv personal communication 26/04/2023;). The bathymetry data were converted to British National Grid with vertical elevations to the Ordnance Datum Newlyn using the OSGM15 model. Prior to further analysis, all raw multibeam soundings collected by the University of Southampton were checked and filtered for outliers within the post-processing software, BeamworX AutoClean (https://www.beamworx.com/). Here, we used a simple 95 % confidence interval filter, meaning that any soundings lying more than two standard deviations from the mean depth within a grid cell (0.5 m) are removed as outliers.

Additional bathymetry profile data were extracted using bilinear interpolation from the NNRCMP/Maritime Coastguard Agency multibeam echosounder survey, carried out 01/08/2013, and from the NNRCMP SBES surveys, recorded on the 04/09/2003 and 12/03/2006 at a resolution of 0.01 m in the cross-shore and ~ 50.0 m in the longshore to ±0.2 m vertical accuracy (Channel Coastal Observatory, 2006; Channel Coastal Observatory, 2003). Raster surfaces for the SBES data were generated through firstly creating a Triangular Irregular Network (TIN) of the SBES points, and then converting the TIN into a raster grid. The bathymetric data are freely available to download from the NNRCMP website, https://coastalmonitoring.org/.

The bathymetry and topographic profiles were initially processed using Python to generate a chainage for each data point, *i.e.* the distance between the data point and the NNRCMP start point of each profile line, which is typically the most landward point of the profile. These processed files were then imported into the beach profile analysis software SANDS (Shoreline And Nearshore Data System, © 2023 Jacobs; see https://www.sandsuser.com/for more information). The software works as a database for topographic beach profile data and was used to quality check the data visually, through inter-survey profile comparison and checking for spikes or irregular surface features, such as those caused by interference from grains of sediment mobilised near the bed by the tide. If any such spikes were found, these were manually deleted (note that this was only for very small, localised areas of one survey). SANDS was then used to combine the topographic and bathymetric profile data creating complete, backshore to offshore, beach profiles (Bradbury et al., 2005). This was done by linking the topographic profile line with the bathymetric profile line, with the bathymetric profile taking precedence in overlapping areas as this data consistently captured a fuller profile at the toe of the beach. The profiles were then interpolated at 1 m spacing with a univariate interpolation, using the Python SciPy module package.

2.2.2. Data analysis

The observational depth of closure method examines variation in elevation between two or more profile surveys, where the depth of closure is found at the point where the absolute difference or standard deviation becomes constant. This represents the survey error and is also known as a non-zero tail (Hinton and Nicholls, 1998). Change above the non-zero tail is considered to be detectable change. Initially, the standard deviation of the elevation was calculated over the range of surveys completed at the three extended profiles. Following this, the absolute difference in elevation was calculated between any two surveys at each chainage point along every profile. From this, the locations of the landward minimum morphological change, apeak morphological

Table 1
Summary of extended profile survey dates and source. Note: N=NNRCMP SBES survey; M = NNRCMP/MCA MBES survey; Px = extended project surveys; P = project surveys.

Location	04/09/2003	12/03/2006	01/08/2013	15/09/2020	30/03/2021	28/04/2021	27/05/2021	15/11/2021	25/11/2021	16/12/2021	25/01/2022	14/04/2022
4c01729 (Westernmost)	N	N	M	Px	Px							Px
4c01727 to 4c01705	N	N	M	P	P							
4c01702 (Central)	N	N	M	Px	Px	P	P	P	P	P	P	Px
4c01699 to 4c01681	N	N	M	P	P							
4c01677 (Easternmost)	N	N	M	Px	Px							Px

change and the depth of closure were identified. The landward minimum morphological change was identified as the first point where conditions meet Kraus et al.'s (1998) guidance "the depth of closure is defined as the most landward depth at which no significant change occurs". The depth of closure was identified as the most seaward point at which no detectable change begins to occur, encompassing all areas of closure and 'reopening' as defined by Hinton and Nicholls (1998). The location of peak morphological change was identified at the cross-shore chainage with the greatest value of absolute difference. The secondary peak was identified to show the largest natural change when this was masked by human interventions to the crest from beach re-profiling. Additionally, the average seabed slope was calculated for profiles between the locations of Mean Sea Level (MSL) and the depth of closure.

2.3. Nearshore transport estimation

To understand the variation in the wave driven processes across the frontage, namely long and cross-shore transport, the wave buoy record (08/07/2003–31/10/2019) was propagated to three nearshore points (located along the three extended profiles) using CoastalTools, an open source, MATLAB based GUI (https://www.coastalsea.uk/). The wave record from the Pevensey Bay wave buoy (Fig. 2) was transformed to give the breaking wave height at the edge of the surf zone using water levels for the same time period from the Newhaven tide gauge (Fig. 2). This was done using linear wave theory, with plane bed refraction and shoaling, together with Weggel (1972) empirical work relating beach slope to breaking wave height as given in eqs. 2–92, 2–93 and 2–94 of the Shoreline Protection Manual (USACE, 1984).

From this inshore transformation of the wave record, both littoral drift potential and cross-shore transport rates were calculated independently for both fine sand (159–164 μm) and medium pebbles (12 mm), using locally derived shoreline angles for each profile. The chosen grain sizes were based on the average of samples collected by Dornbusch et al., 2005a,Dornbusch et al., 2005b for the upper beach and using samples of the sandy foreshore as described in Section 2.4 Sediment analysis. Cross shore transport rates were estimated using Bailard and Inman (1981), accounting for both the suspended and bed loads. Longshore transport rates were estimated using Damsgaard and Soulsby (1996) for the medium pebbles, a physics based equation used to predict longshore bedload transport, calibrated against a 3 year field dataset of longshore sediment transport on a shingle beach in the south of the UK. Finally, the simplified version of the CERC equation (which does not take into account bed slope nor grain size), *i.e.* the SANDS formula, was utilised to represent sand transport (Soulsby, 1997). The full equations for the wave transformation and sediment transport are provided within the supplementary information.

2.4. Sediment analysis

Eight van Veen grab samples were retrieved at the locations of an instrument array of benthic landers on the 04/07/2022 and the 07/09/2022 (locations shown with white circles in Fig. 2). As work by Dornbusch et al., 2005a,Dornbusch et al., 2005b did not provide information on the sandy foreshore, samples were also taken from this zone on the 19/11/2019. Grain size analysis was completed complying to BS EN ISO 17892-4:2016. Using the arithmetic method of Krumbein and Pettijohn (1938), the textural statistics were calculated, namely median grain size, sorting, skewness and kurtosis.

2.5. Sediment balance

To better understand the observed chronic loss of sediment at Pevensey Bay (Thomas, 2015) change in upper beach profile slope (Section 2.5.1) and cross sectional area of the nearshore over time were analysed (Section 2.5.2).

2.5.1. Upper beach slope analysis

Change in the lateral position of MSL is not natural at Pevensey Bay as the gravel barrier is maintained to a design width. However, the beach slope is not maintained (despite small amounts of reprofiling after the placement of recycled/recharge material) which means that long-term rotational movement of the cross-shore intertidal profile, *i.e.* steepening/flattening, can be examined. This was done by analysing the relative positional changes of mean low water and mean high water which were extracted for each NNRCMP beach profile, following Taylor et al.'s (2004) method. The changes were calculated for each spring topographic survey from 2003 to 2022 carried out by the NNRCMP. Specifically, Mean High Water Neap (MHWN) and Mean Low Water Neap (MLWN) elevations were used to allow the widest coverage across the bay as some NNRCMP profiles did not extend down to the Mean Low Water Springs (MLWS).

2.5.2. Nearshore cross-sectional area

The cross-sectional area above the datum −12.0mOD for which all bathymetric surveys covered was calculated for each profile (Fig. 2, Table 1). This analysis was carried out in the software SANDS. The results of this analysis provide an indication of the volume of material across the bay over the time periods where data were available (Table 1).

3. Results

3.1. Depth of closure – Wave energy approach

The predicted depth of closure ranged between − 8.03 and − 11.02 m Ordnance Datum (OD) for the inner closure depth representing seasonal change, and − 12.94mOD for the outer limit (Table 2).

3.2. Depth of closure – Observational approach

Historic and repeat surveys of the Central profile 4c01702 indicate the level and extent of bed elevation change over different timescales (Fig. 3). Subplot A of Fig. 3 illustrates the profile surveyed at different time periods and shows the steeper upper beach located within the first 100 m chainage, and the flatter shoreface slope seawards beyond this. The absolute difference in bed elevation between surveys shows change occurring over the full extent of the surveyed area over longer timescales (greater than six months (Fig. 3, subplot E and H) to years (Fig. 3, subplots B to D)), whereas analysis of shorter timescales (less than three months, Fig. 3, subplot F, G, I to L) shows change limited to certain areas at approximately 300 m, 600 m and 950 m offshore. These changes are caused by the apparent progressive onshore movement of bar features over the course of a year. Multibeam bathymetry and X-band radar reflectance imagery have shown that these are transverse finger bars, which lie at ~45 degrees to the coastline and are moving easterly at a rate of approximately 100 m a^{-1} (Townsend et al., 2023). Over longer timescales (subplots B—D) changes occur up to the survey limit (1 km offshore) and therefore the depth of closure may be further offshore. The short spike in the absolute difference at approximately 30 m chainage is

Table 2
Results from wave statistics and depth of closure.

Description	Value	Units
Wave statistics		
He	3.68	m
Te	6.23	s
Depth of closure results		
Hallermeier	−9.60	mOD
Hallermeier simplified	−11.02	mOD
Birkemeier	−8.03	mOD
Birkemeier simplified	−9.43	mOD
Hallermeier outer	−12.94	mOD

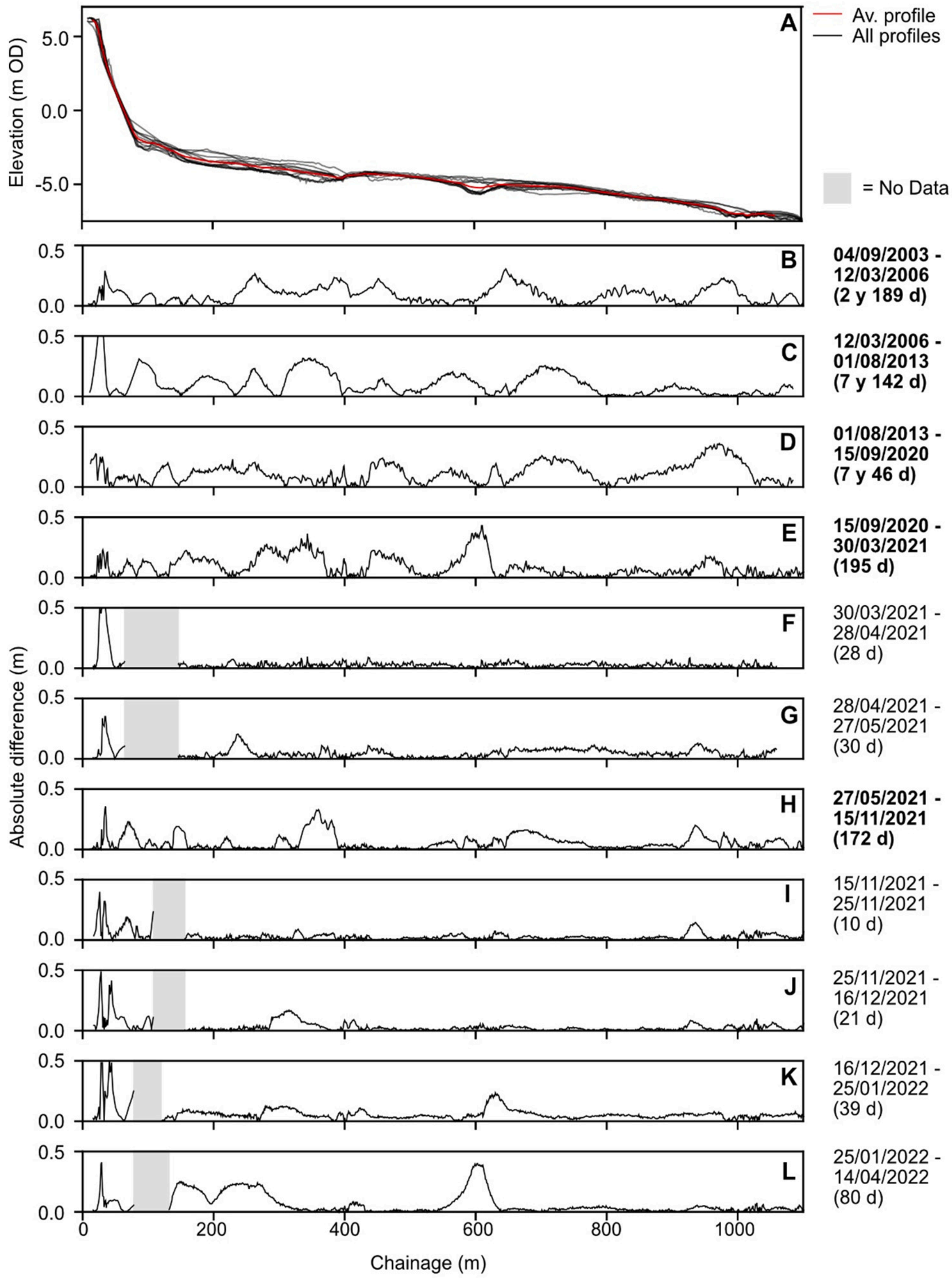

Fig. 3. Mean profile and surveyed cross section of Central profile 4c01702 (A) and elevation variation between surveys, 04/09/2003 to 25/01/2022 (B to L). Sections with no data shown in grey, where topographic and bathymetric surveys did not overlap fully. The duration between the two surveys is indicated in parentheses. Time periods approaching 6 months and greater highlighted in bold.

caused by the change in crest position, from erosion and cliffing events, as well as *ad hoc* beach recycling to maintain the width of a haulage route which runs between the barrier crest and a row of beachfront properties.

We used the absolute difference between the bed level change for the 2020 Autumn and 2021 Spring surveys to capture the change caused by winter storms (Fig. 4). The landward minimum morphological change was found to be shallower than the Lowest Astronomical Tide (LAT) for 11 out of 18 profiles, but for some profiles in the east, this depth was below LAT. The intertidal area is roughly the same width throughout the study site, whilst the deeper contours of − 5.0 and − 6.0 mOD show that the shoreface is steeper in the west, closest to Sovereign Harbour, but flattens out and becomes shallower, towards the east. The depth of closure follows this pattern, moving further offshore as the bed slope decreases to the east. The location of peak morphological change for nearly all the profiles west of the Central profile 4c1702 is above MSL, around the barrier crest, possibly in response to beach reprofiling works. To the east of the Central profile (4c01702), the peak morphological change is found to be much greater than in the west and further offshore in water depths greater than the − 5.0mOD contour.

3.3. *Depth of closure – Wave energy vs observational approach*

The observed depth of closure for the study site is shallower than the predicted depths estimated using the Hallermeier and Birkemeier equations (Fig. 5, eqs. 1–4), but the Birkemeier equation (eq. 3) provides the best estimate of closure depth. Over a 9 year timescale, the observed depths of closure were within 0.23 m on average of the Birkemeier equation (eq. 3), but ranged on average from 1.63 m, 1.80 m and 3.22 m shallower for the simplified Birkemeier, Hallermeier and simplified

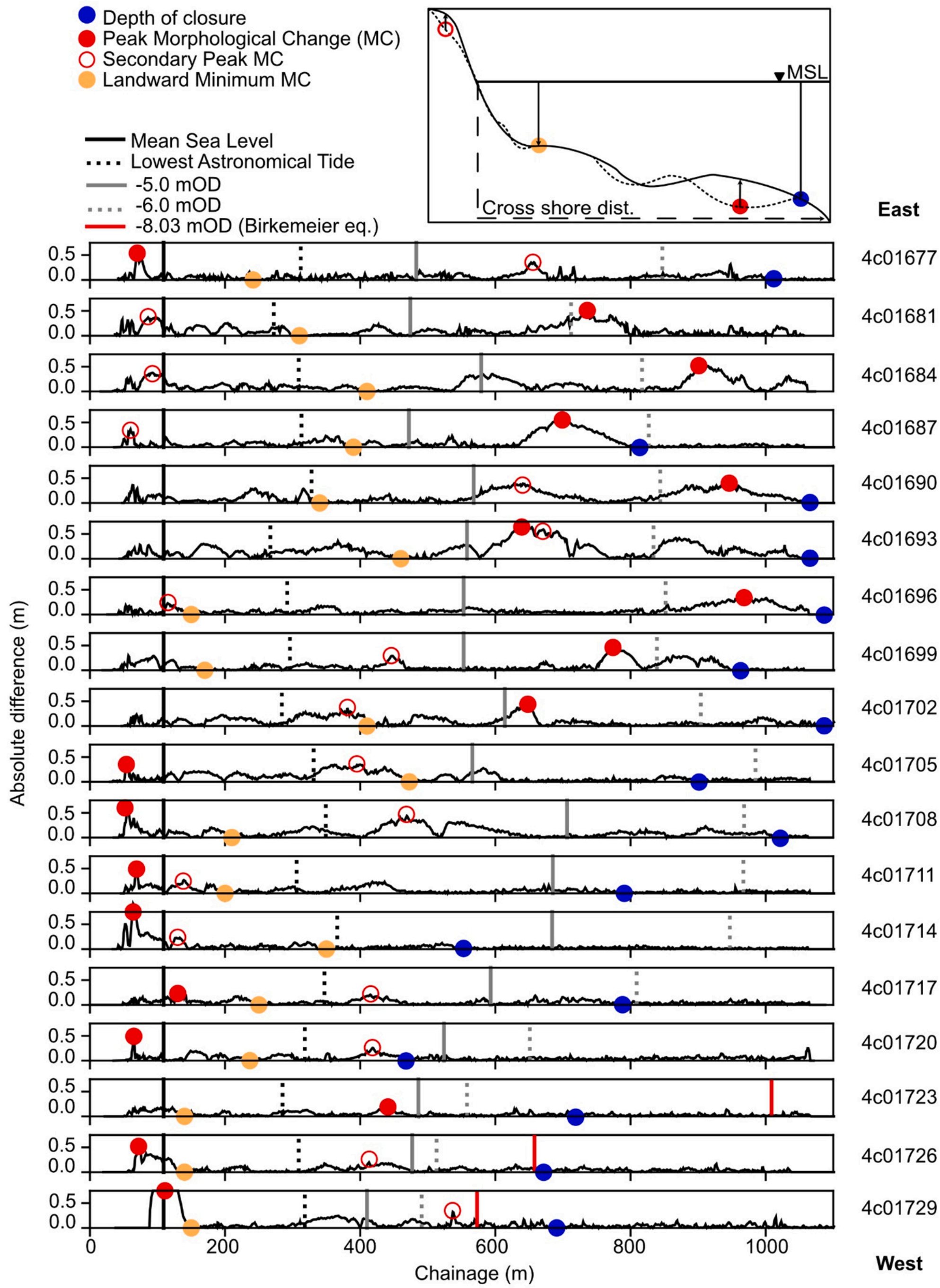

Fig. 4. Top right) Depth of closure, alongside peak, secondary peak and landward minimum morphological change with 0 mOD reference point for measuring cross shore distance. Main figure) Absolute difference between Autumn 2020 and Spring 2021 'bay wide' surveys. All profiles plotted relative to the 0 mOD contour chainage, representing Mean Sea Level (shown as thick black vertical line). Dashed black, solid grey and dashed grey vertical lines show the position of the LAT (−3.65mOD), -5mOD and -6mOD contours respectively. N.B. large variation at 100 m chainage on Westernmost profile 4c01729 is due to beach management activities.

Hallermeier equations (eqs. 4, 1 and 2) respectively (Fig. 5, Panel A). Over a single winter period the observed depth of closure ranged between 0.37 deeper and − 3.33 m shallower than the Birkemeier equation (Fig. 5, panel B).

The variations in nearshore waves, bed slope and surface roughness across the frontage are presented against the observational depth of closure in panel A of Fig. 5. The indicative bed type shows that the predominant surficial sediment type across the bay's nearshore is sand, and that nearshore morphology becomes more dynamic eastwards. Westernmost profile 4c01729 is noticeably steeper than the other profiles and fronted by a planar bed of mixed sediment. Changes in bed elevation appear to be limited to a nearshore bar, located at around 450 m offshore. Notably, the annual beach recharge (~20,000m^3 material) is deposited here, which is evident in the most shoreward part of the profile, between surveys in 2020 (just after nourishment) and 2021 (after winter storms/erosion). There are extensive areas of gravel along the Central profile, 4c01702, which do not seem to inhibit bed movement overtime. However, there appears to be an area which has experienced very little bed elevation change at approximately 400 m offshore. The elevation of the areas identified as rocky outcrops in the

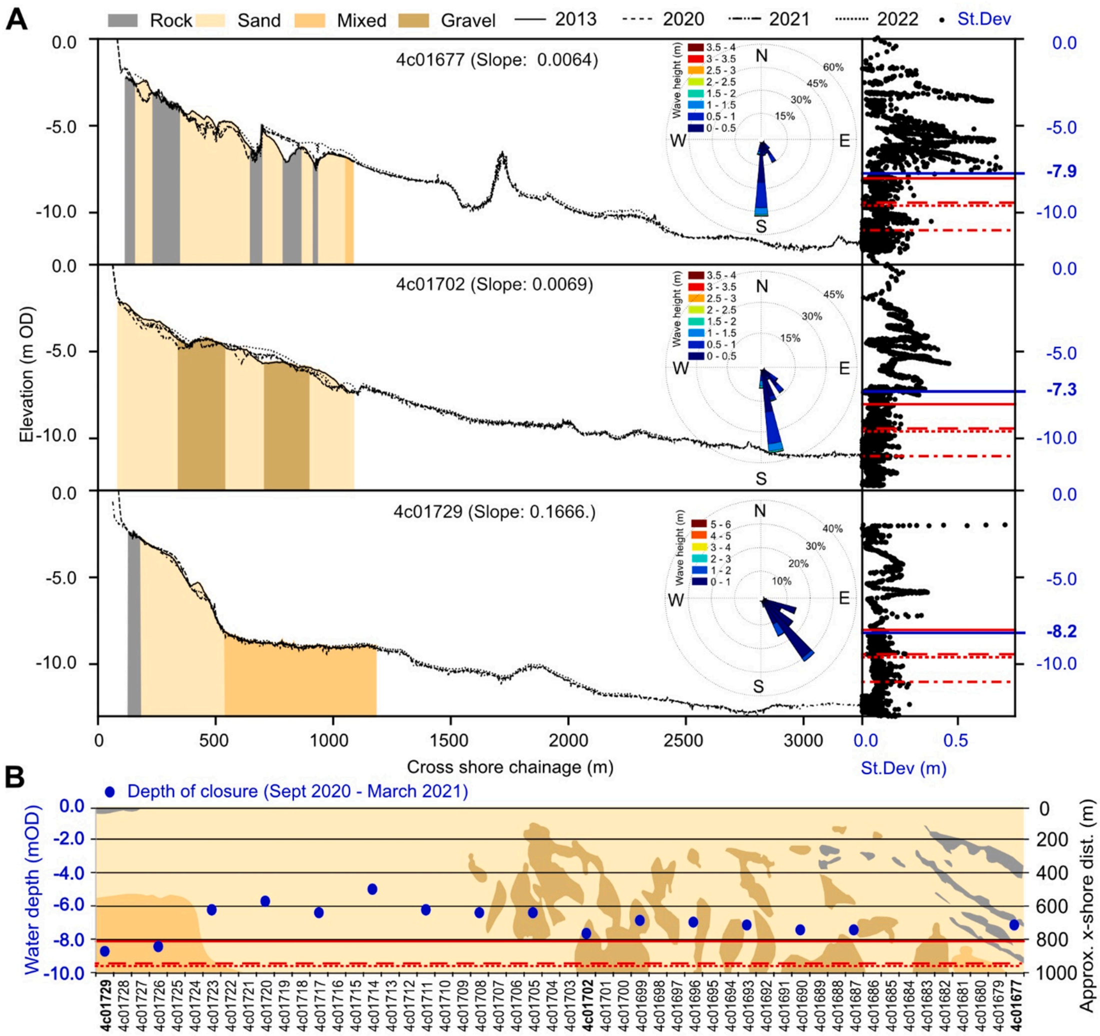

Fig. 5. Variation of the three extended cross-shore profiles (Easternmost: 4c01677, Central: 4c01702 & Westernmost: 4c01729) through time. The standard deviation of bed level *vs* depth is shown, together with the observational depth of closure (blue lines, *i.e.* when SD reaches a constant non-zero tail, which is around 0.15 m for this dataset) and the predicted depth of closure (red bars, namely Birkemeier (−8.03 mOD, solid red), simplified Birkemeier (−9.43 mOD, dashed red), Hallermeier (−9.60 mOD, dotted red) and simplified Hallemeier (−11.02 mOD, dash-dot red). The slope between MSL and the observed closure depth is also given with the profile name label. Indicative bed composition from the 2013 backscatter interpretation is also shown, as gravel, sand, mixed and rock (N.B. this method cannot detect mud). The inset roses show propagated nearshore wave record for each beach profile derived from CoastalTools. (For interpretation of the references to colour in this figure legend, the reader is referred to the web version of this article.)

Easternmost profile 4c01677 typically does not change over time, except for two areas which were exposed in 2013 but subsequently buried, around 300 and 800 m offshore.

Panel B shows the depth of closure to be at its shallowest around Profile 4c01714, becoming progressively deeper in both directions away from this minimum. From the Central profile 4c01702 eastwards, the depth of closure is relatively stable with the exception of two profiles, 4c01684 and 4c01681, where closure did not occur within the 1 km survey area. The area in which the depth of closure becomes shallower (Westernmost profile 4c01729 to 4c01714) correlates with an increasingly wide nearshore zone shown by the position of the −5.0 mOD contour (Fig. 4); and a reduction in bed slope from the steepest Westernmost profile 4c01729, which was two orders of magnitude greater than the Central (4c01702) and Easternmost (4c01677) profiles (Fig. 5, panel A). East of Profile 4c01714, the bed slope is relatively constant (Fig. 5) and so cannot explain variations in the depth of closure in this area.

3.4. Nearshore transport estimation

The estimated volumetric sediment transport rates suggest that easterly longshore transport is dominant, being an order of magnitude greater than westerly transport, and two to three orders of magnitude greater than cross shore transport (Fig. 6). As different longshore sediment transport equations are used for the fine and coarse fractions, the results are not directly comparable. However, these indicatively suggest that the transport rate of sand may be up to one order of magnitude greater than for the coarse sediment. The gradient in longshore transport rate shows a west to east transition from a more erosive environment to a depositional environment.

3.5. Sediment analysis

The sediment sampling which took place along the central profile (Fig. 2) showed that mud is abundant within the nearshore sediments of Pevensey Bay (Table 3). The sample types varied from unimodal to polymodal and were typically very poorly sorted, but occasionally moderately sorted. The mud content of the total sample weight varied

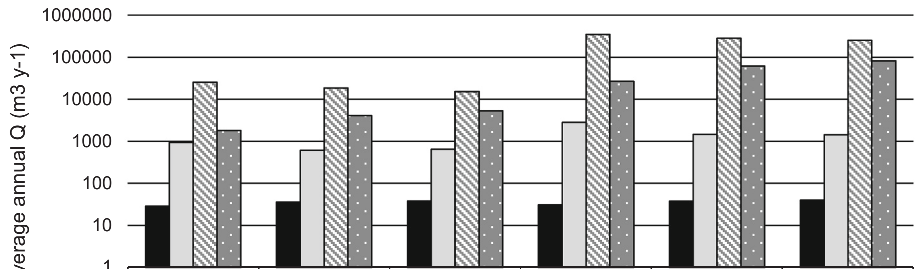

	4c01729 - Coarse	4c01702 - Coarse	4c01677 - Coarse	4c01729 - Fine	4c01702 - Fine	4c01677 - Fine
Onshore	28.70	35.90	38.00	30.70	37.50	40.10
Offshore	931.20	614.70	646.00	2,815.80	1,463.40	1,424.10
Easterly	25,547.50	18,520.70	15,332.40	349,253.40	283,773.00	253,704.80
Westerly	1,815.20	4,102.80	5,377.80	26,775.90	62,388.00	82,932.60

Fig. 6. Estimated long and cross shore sediment transport approximated on the beach face at the Westernmost (4c01729), Central (4c01702) and Easternmost (4c01677) profiles. Cross-shore transport is estimated using Bailard and Inman, (1981) whilst longshore transport is estimated using Damsgaard and Soulsby (1996) and Soulsby, (1997) for the coarse (medium pebble, 12 mm) and fine (fine sand, 161.5 μm) fractions, respectively.

Table 3
Mud, sand, gravel ratios by weight taken from samples at the instrumented array.

	West array				*East array*			
Metres offshore	% mud	% sand	% gravel	Class	% mud	% sand	% gravel	Class
July sample								
500	5	95	0	Sand	7	92	1	Sand
1100	6	94	0	Sand	30	70	0	Sandy mud
1700	5	65	30	Gravelly Sand	27	73	0	Sandy mud
2300	7	93	0	Sand	8	78	14	Gravelly sand
September sample								
500	31	69	0	Muddy sand	35	65	0	Muddy sand
1100	34	66	0	Muddy sand	53	47	0	Sandy mud
1700	64	36	0	Sandy mud	73	27	0	Sandy mud
2300	21	79	0	Muddy sand	2	98	0	Sand

between 5 and 30 % with an average of 12 % mud content in July, and 2–73 % with an average of 39 % in September. Small amounts of gravel were present in the grabs recorded in July, supporting the backscatter substrate mapping shown in Fig. 5. However further samples taken in the winter months may confirm this as fine material allowed to settle out in the summer months is resuspended.

3.6. Sediment balance

The majority of the beach profiles have experienced steepening between 2003 and 2022 (Fig. 7, panel B). East of Profile 4c01719, the steepening was typified by the landward retreat of the MLWN mark (averaging ~15 m with a peak value of nearly 40 m), and a relatively stationary MHWN mark (±5 m change), most likely due to the beach management activites work to maintain the position of the crest. West of Profile 4c01719, the changes in MHWN and MLWN were generally of a smaller magnitude and showed retreat, suggesting regression of the shoreline in this area. The bay planform is of a typical embayment, with the beach orientation becoming aligned with oncoming wave crests with increased distance from the fixed 'headland' at Sovereign Harbour. The beach orientation is also shown on Fig. 7, panel A. The shoreline orientation suggests a switch from beach profile regression to steepening as the beach orientation becomes greater than ~30^{o}N. Overall changes in the cross-sectional area of the nearshore overtime suggest loss of sediment across the bay (Fig. 7, panel C). Although the error is realtively high, consistent loss over the years across the bay suggest a clear trend.

4. Discussion

Heterogenous, mixed sediment environments have a variable depth of closure which varies spatially due to the distribution of sediments and variations in grain size. In a controlled environment, mixed sediments are likely to contribute to a shallower depth of closure, and lower bed elevation change in comparison to an equivalent 'pure sand' setting due to a higher critical threshold for motion, related to increased sediment size, the shielding of finer sediments and/or the cohesive effects of muds and clays. When compared to the predictive equations, the observed depths of closure were consistently shallower, however, results indicating a shallower observed depth of closure are common (Barrineau et al., 2021) and explanations include: 1) 'real-world' conditions never reaching an equilibrium state due to non-stationarity; 2) constraining geology; and 3) bathymetry surveys not capturing the greatest change, as the profile of the seabed recovers after the peak of the storm (Robertson et al., 2008).

The interpretation of the variation in the depth of closure at complex sites such as Pevensey can be assisted through systematic assessment of the physical parameters outlined in Fig. 1, namely 1) bed slope, 2) bed resistance, and 3) hydrodynamics.

At Pevensey, changes in the depth of closure were likely related to the availability of mobile sediment and bed slope. The gradient of the longshore transport rate (high to low moving west to east) results in a transition from a more erosive to more depositional environment. We postulate that as hydrodynamic conditions become more conducive to deposition, there is greater sediment availability (mainly in the form of bedform features) and that this contributes to a deeper depth of closure in this area. The impacts of this progression explain the increase in bed elevation change from west to east (Fig. 4) as the increased likelihood of deposition leads to sediment available for mobilisation. Additionally, each year approximately 20,000 m^3 of sediment is placed at the Westernmost (4c01729) profile locally increasing the volume of available

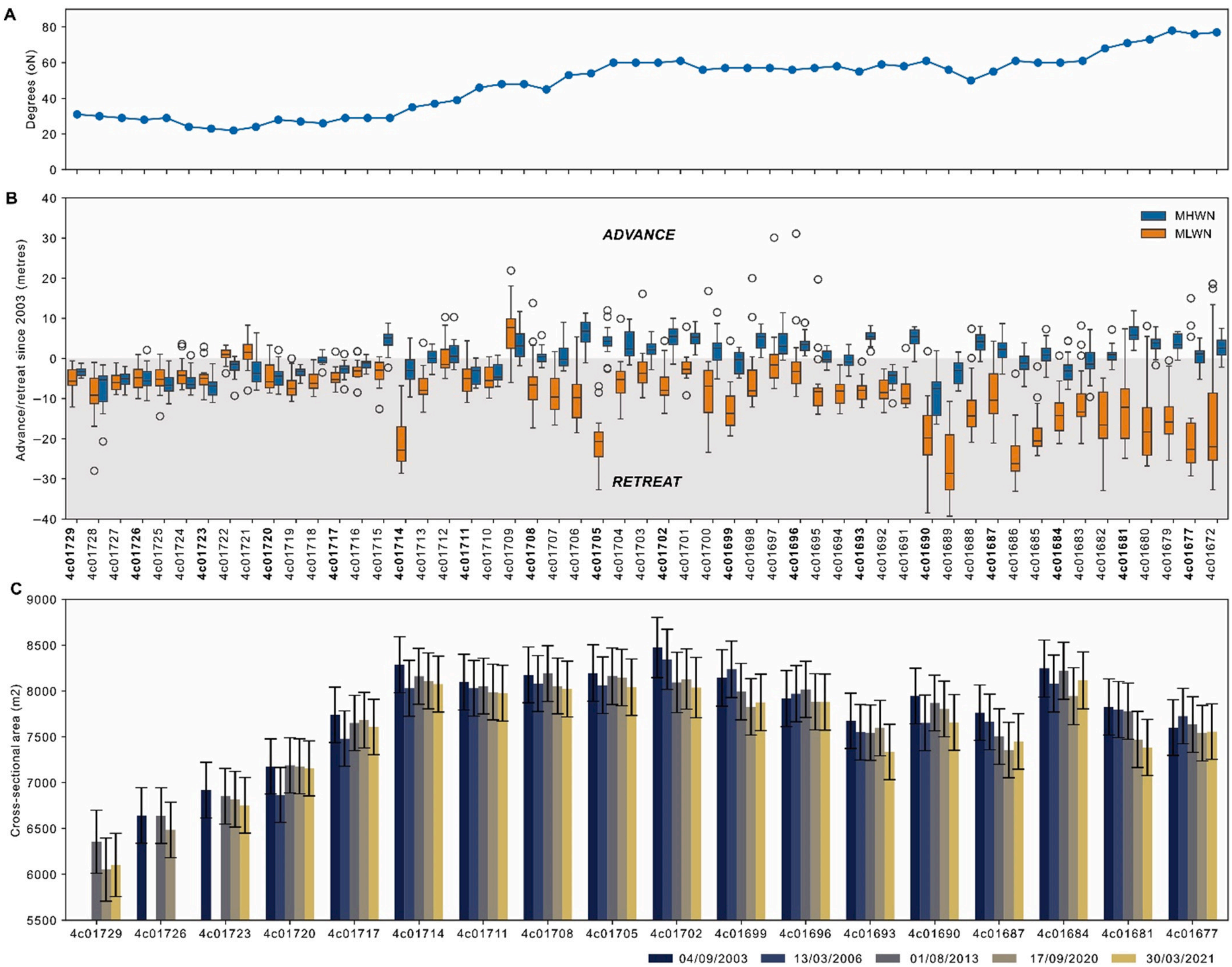

Fig. 7. NNRCMP beach profile locations showing A) Shoreline orientation relative to degrees north (°N) where a beach facing South would be 90°N, whilst a beach facing North would be 270°N; B) Change in lateral position of MHWN and MLWN relative to their position in 2003, with outliers shown as white dots; and C) the cross sectional area for the 18 surveyed profiles displayed with error bars showing the upper error estimate of ±0.3 m multiplied by the length of the profile to give areal error.

sediment. These observations go some way to explaining the variations in the depth of closure within the study site, which was shown to decrease in depth from west to east between the Westernmost (4c01729) profile and profile 4c01714, and then gradually deepen from the minimum at 4c01714 towards the Easternmost (4c01677) profile. It is also thought that the very steep nearshore slopes in the very west of the frontage (Westernmost profile 4c01729 to 4c01723) may contribute to a deeper closure depth at this location, due to greater offshore transport. The indicative bed type did not help explain variations in the depth of closure. Notably the shallowest depth of closure was observed in a purely sandy area, whilst the areas with gravel outcrops were up to ~3 m deeper over the short term (Fig. 5, panel B). This may be due to the fact that the gravel beds only make up a small percentage of the total bed material in this area, and we postulate that the observed depth of closure is dependent on the modal or smallest sediment size, rather than the larger grain sizes. The influence of cohesive sediments at Pevensey is not understood, as the sediment sampling showed that the distribution of mud varied widely in both space and time. It is likely that the cohesive sediments are exerting some form of control, as the effects of mud strengthening bed resistance have been observed with thresholds as low as 3–18 % in sand mud environments (Mitchener and Torfs, 1995), and they were found to average 12 to 39 % at the study site. However, the cohesiveness of the muds will also be influenced by their mineral composition, water content and whether any biofilms were present (Grabowski et al., 2011; Jacobs et al., 2011). These factors could play an important role in the dynamics of mixed sediment nearshore environments, and further work is required to understand both the wider spatial distribution and the effects on bed mobilisation.

The exploration of the nearshore zone of this mixed sediment environment using observational data, brought to light three specific findings which may be applicable to sites of a similar nature:

1. Low magnitude observed bed elevation change: The site generally experiences very low magnitude bed elevation change across the frontage, which does not increase over the medium term (19 years of data). For instance, between the Autumn 2020 and Spring 2021 surveys bed elevation change across the frontage typically ranged between 0.1 and 0.6 m, only exceeding this at the Westernmost profile, 4c01729, following a beach recharge (Fig. 4). At the Central profile 4c01702, the bed levels across the subtidal profile were shown to consistently fluctuate between 0 and 0.3 m over the longer time periods (~6 months and greater), and at the shorter time intervals changes related to the transverse bars could be seen (Fig. 3), suggesting that the bed elevation change is tied to the amplitude of these bedforms. This is a problem for detecting the depth of closure using a survey error threshold approach, such as that employed by Pagán et al. (2017), as there is a reasonable chance that the maximum survey error threshold (±0.3 m) may not be exceeded. Using the absolute survey difference, or standard deviation between more than two surveys to find the depth of closure from the non-zero tail was a suitable alternative to this.

2. Wave driven morphodynamic change: Spikes in bed elevation change, found around the 300 m, 600 m and 950 m chainage show that sediments are mobile across this area, which are due to the infilling of troughs as a transverse finger bar system moves alongshore (Fig. 3; Townsend et al., 2023). Fig. 3 also shows that there is no bed change in these areas during the summer, which suggests this movement is seasonal and driven by waves, not tidal currents. To successfully capture the lower limit of this active area, it was necessary to ensure all areas of reopening were captured above the depth of closure as the landward minimum morphological change, was found in much shallower water. It is unknown why there is an area of minimum morphological change in this area, between larger magnitude changes on the upper mixed gravel sand beach and further offshore. However, we postulate that the peak changes are related to the different sediment fractions response to waves, with the offshore peak morphological change linked to a more mobile sandy bed, whilst the changes in the upper beach reflect berm movement, either by waves or through beach management activities. Between these two peaks sits the landward minimum morphological change, representing an area which is relatively stable in comparison to the changes around it.

3. Peak morphological change. The identification of the location of peak and secondary peak morphological change, show that the largest volumes of bed level changes are primarily found offshore, between the −5.0 and − 6.0 mOD depth contours, located approximately 0.4 to 1.0 km offshore. Greater variation in bed elevation across nearshore profiles was found towards the east (Fig. 4); suggesting that there is more sediment availability and mobility on a wider nearshore platform. This agrees with the work of Hamon-Kerivel et al. (2020) who classified the shoreface based on sediment availability. The upper, reflective part of the beach was also highlighted as a key area of change. Although without the active recycling works and artificial import of sediment countering erosion, the changes in this area could be far larger.

Long term loss of sediment was observed across the nearshore since 2003, which is concurrent with the findings of Thomas (2015) who found loss of intertidal sediment below MSL between 2003 and 2015. The losses observed across the nearshore equate to small changes in elevation, but over a much larger area, are vast in comparison to the observed changes in the upper beach sediments, something that was also highlighted by the analysis of the location of the peak morphological change. The beach management efforts at Pevensey are effectively locking the shoreline in place, leading to coastal steepening along two thirds of the beach profiles (Fig. 7). The loss of volume of nearshore sediment is most likely due to the dominant easterly transport (Fig. 6) with limited supply of sediment from the west. Littoral drift analysis showed shingle volumes that were comparable to those deducted from a regional sediment budget for the upper beach (Environment Agency, 2015) however, the sand volumes, which were an order of magnitude larger, remain unvalidated. Should the changes observed in the nearshore and lower intertidal area continue, increases in wave power reaching the shore may be expected, compounding the effects of sea level rise. Dornbusch (2017) showed that to prevent the drowning of 190 km gravel barrier beaches in the South East of the UK (including Pevensey Bay) from sea level rise, increases in barrier crest height, and therefore upper beach volume, and longshore transport control measures would be required, resulting in significant increases to cost. The beach management activities which are undertaken today counteract the ongoing loss of upper beach (mainly coarse) sediment from the study area but they do not address the long-term loss of nearshore sediments. Unless the upper beach can be allowed to migrate landward and form a more natural profile, the beach could be expected to continue to move towards a maximum steepness, leading to increased wave reflection and ongoing loss of fines from the foreshore and requiring increased engineering intervention to prevent drowning/breach of the shingle barrier.

Further work is needed to understand the nearshore zone and quantify its changing behaviour on the current shoreline policy of hold the line. To aid in this advance, we make the following recommendations. Firstly, it is imperative that greater assurance is gained from bathymetric data to help inform management decisions. Currently, bathymetric data is generally quoted as having ±0.3 m vertical accuracy, which encompasses composite error from both the sonar instrumentation, Inertial Motion Units and positional error (from Global Navigation Satellite System). Secondly, this work has shown the importance of the nearshore to the upper beach sediments, and therefore strategic coastal monitoring should adapt to take these findings into account. Finally, the interpretation of the backscatter imagery from the 2013 multibeam survey and sediment samples taken from the array area showed a highly variable spatial and temporal distribution of sediments. From the information we have at present we cannot derive an accurate picture of how the bed changes overtime and whether the changes observed are the result of loss of fines, or whether coarser material is also being lost. Therefore, to better understand the resilience of this shoreline, a better understanding of the sediments distribution through space and time should be gleaned.

5. Conclusions

This paper examines the relationship between the effects of shoreline management on beach steepening and the nearshore zone; using the bed elevation change and the depth of closure to describe the extent and behaviour of the active nearshore zone. Comparisons were made between observed and predicted depths of closure, finding that the Birkemeier equation was the closest approximation for a lower limit of change, yet, variation was found between the observed and predicted depths across the site at both seasonal (differences between 0.37 m deeper and 3.33 m shallower) and decadal (differences between 0.17 m deeper and 0.73 m shallower) timescales. A conceptual model outlining the physical parameters that influence the depth of closure was used to systematically interpret the variations seen across the site. The need for a greater understanding of sediment grain size, including cohesive sediments was highlighted, as sampling from one location revealed high temporal and spatial variability in mud content which is known to affect the mobilisation of sediments. Three further findings specific to the site but of potential interest to other mixed sediment sites were also made: 1) the seabed elevation change is very low (typically *c.* 0.3 m, the same magnitude as the upper limit for survey error) and thought to be limited in some locations to the amplitude of the bedforms in the area; 2) the magnitude of changes in seabed elevation varied over short timescales, suggesting, as could be expected, most change occurred during the winter months or post storm activity; and 3) it is thought that there is a relationship between the magnitude of the most seaward peak or secondary peak morphodynamic change (ignoring changes to the upper beach) and the width of the nearshore zone, implying that the wider nearshore zone has more freely available sediment. Finally, the long-term changes to the upper beach profile were considered in relation to the nearshore. It was found that coastal steepening had occurred to over two thirds of the beach profiles and that the cross-sectional area of the nearshore zone had also decreased over time, which could both contribute to increased need for beach management activities in the future, although the effects are currently unquantified.

CRediT authorship contribution statement

Dominique Townsend: Writing – original draft, Visualization, Methodology, Investigation, Formal analysis, Conceptualization. **Julian Leyland:** Writing – review & editing, Methodology, Conceptualization. **Hachem Kassem:** Writing – review & editing, Methodology, Conceptualization. **Charlie Thompson:** Writing – review & editing, Methodology, Conceptualization. **Ian Townend:** Writing – review & editing, Methodology, Conceptualization.

Declaration of competing interest

The authors declare that they have no known competing financial interests or personal relationships that could have appeared to influence the work reported in this paper.

Data availability

Data will be made available on request.

Acknowledgements

This work was supported by the Environment Agency through the project: "Delivering Legacy from the Pevensey Bay Coastal Defence Scheme (PI: Kassem, H.; Contract: 201-09-SD10). The lead author undertook this work as part of their PhD studentship, funded by NERC INSPIRE DTP (NE/S007210/1), the Graduate School of the National Oceanography Centre, Southampton, and the Environment Agency. Our thanks also go to Ian Thomas and Amber Carr of Pevensey Coastal Defence Ltd., and Peter Amies and Rebecca Manning of the Environment Agency for their time, on-site support, and site background information. Further thanks go to those involved with the National Network of Regional Coastal Monitoring Programme for England, in particular Dan Amos of Adur-Worthing Councils and Stuart McVey of New Forest District Council.

Appendix A. Supplementary data

Supplementary data to this article can be found online at https://doi.org/10.1016/j.geomorph.2024.109150.

References

Anthony, E.J., Aagaard, T., 2020. The lower shoreface: Morphodynamics and sediment connectivity with the upper shoreface and beach. Earth-Science Rev. 210, 103334 https://doi.org/10.1016/j.earscirev.2020.103 334.

Aragonés, L., López, I., Villacampa, Y., Serra, J.C., Saval, J.M., 2015. New Methodology for the Classification of Gravel Beaches: Adjusted on Alicante (Spain). J. Coast. Res. 314, 1023–1034. https://doi.org/10.2112/jcoastres-d-14-00140.1.

Aragonés, L., Pagán, J.I., López, I., Serra, J.C., 2018. Depth of closure: New calculation method based on sediment data. Int. J. Sediment Res. 33, 198–207. https://doi.org/10.1016/j.ijsrc.2017.12.001.

Aragonés, L., Pagán, J.I., López, M.P., Serra, J.C., 2019. Cross-shore sediment transport quantification on depth of closure calculation from profile surveys. Coast. Eng. 151, 64–77. https://doi.org/10.1016/j.coastaleng. 2019.04.002.

Ashton, A.D., Murray, A.B., 2006. High-Angle Wave Instability and Emergent Shoreline Shapes: 2. Wave Climate Analysis and Comparisons to Nature High-angle wave instability and emergent shoreline shapes: 2. Wave climate analysis and comparisons to nature. doi:https://doi.org/10.1029/2005JF000423.

Bailard, J.A., Inman, D.L., 1981. An energetics total load sediment transport model for a plane sloping beach: local transport. J. Geophys. Res. Ocean. 86, 2035–2043.

Barrineau, P., Janmaat, R., Kana, T., 2021. Empirical depths of closure along the US East coast. Coast. Eng. 170, 104009 https://doi.org/10.1016/j.coastaleng.2021.104009.

Birkemeier, W.A., 1985. Field data on seaward limit of profile change. J. Waterw. Port, Coastal, Ocean Eng. 111, 598–602. https://doi.org/10.1061/(asce)0733-950x(1985)111:3(598).

Bradbury, A.P., Mason, T., Barter, P., 2005. Large-scale multi-agency strategic beach monitoring of the South-East Coast of England – provision of data and analytical tools. Proc. 2005 Natl. Conf. Beach Preserv. Technol. 44, 1–16.

Brutsché, K.E., Iii, J.R., Pollock, C.E., 2015. Calculating Depth of Closure Using WIS Hindcast Data. Erdc/Chl Chetn VI, p. 11.

Channel Coastal Observatory 2003. Metadata for Hydrographic Survey, ID: 64856.

Channel Coastal Observatory, 2006. Metadata for Hydrographic Survey, ID: 91125.

Channel Coastal Observatory, 2014. Seabed Mapping. Dungeness to Selsey.

Damsgaard, J.S., Soulsby, R.L., 1996. Longshore bed-load transport. In: 25th International Conference on Coastal Engineering, pp. 3614–3627.

Dornbusch, U., 2017. Design requirement for mixed sand and gravel beach defences under scenarios of sea level rise. Coast. Eng. 124, 12–24. https://doi.org/10.1016/j.coastaleng.2017.03.006.

Dornbusch, U., Hardiman, N., 2020. Disappearing beaches? Examples of their increasing replacement in Great Britain by hard structures and non-cohesive sediment accumulations. Coastal Management 2019, 347–360. https://doi.org/10.13140/RG.2.2.32554.77760.

Dornbusch, U., Watt, T., Williams, R.B.G., 2005a. Sedimentary structure of mixed sand and shingle beaches : preservation potential and environmental conditions. INQUA-IGCP 495 Meet. Late Quat. Coast. Chang. sea level, Sediment. forcing Anthropog. Impacts 19–20.

Dornbusch, U., Williams, R., Moses, C., 2005b. Beach Materials Properties. BAR Phase 1,. Science Report.

Dumas, S., Arnott, R.W.C., 2006. Origin of hummocky and swaley cross-stratification - the controlling influence of unidirectional current strength and aggradation rate. Geology 34, 1073–1076. https://doi.org/10.1130/G22930A.1.

de Figueiredo, S.A., Goulart, E.S., Calliari, L.J., 2020. Effects of closure depth changes on coastal response to sea level rise: Insights from model experiments in southern Brazil. Geomorphology 351, 106935. https://doi.org/10.1016/j.geomorph.2019.106935.

Elsner, P., Dornbusch, U., Thomas, I., Amos, D., 2015. Monitoring mixed sand and gravel beaches using unmanned aerial systems. In: Wang, P., Rosati, J.D., Cheng, J. (Eds.), Coastal Sediments 2015: The Proceedings of the Coastal Sediments 2015. World Scientific Publishing, ISBN 9789814689984.

Environment Agency, 2015. Regional Beach Management Plan Eastbourne to Rye.

Francois, S., Stive, M.J.F., Pons, F., 2005. Longshore Variation of Depth of Closure on a Micro-Tidal Wave-Dominated Coast 2327–2339. https://doi.org/10.1142/9789812701916_0187.

Fugro Emu, 2016. Pevensey Bay, South-East England. Hydrodynamic Study ADP Investigation Report.

Grabowski, R.C., Droppo, I.G., Wharton, G., 2011. Erodibility of cohesive sediment: the importance of sediment properties. Earth-Science Rev. 105, 101–120. https://doi.org/10.1016/j.earscirev.2011.01.008.

Hallermeier, R.J., 1977. Calculating a Yearly Limit Depth to the Active Beach Profile, Techical Paper Coastal Engineering Research Centre. Ft, Belvoir, Va.

Hallermeier, R.J., 1978. Uses for a calculated Limit Depth to Beach Erosion. Proc. Coast. Eng. Conf. 2, 1493–1512. https://doi.org/10.9753/icce.v16.88.

Hallermeier, R.J., 1981. Seaward limit of significant sand transport by waves: an annual zonation for seasonal profiles. No. CERC-CETA-81-2. Coast. Eng. Res. Cent. FORT BELVOIR VA, 1981. Eng. Res. Cent. FORT BELVOIR VA.

Hallermeier, R.J., 1983. Sand transport limits in coastal structure designs. In: Conference on Design, Construction, Maintenance and Performance of Coastal Structures, pp. 703–716. ASCE, Arlington.

Hamon-Kerivel, K., Cooper, A., Jackson, D., Sedrati, M., Guisado Pintado, E., 2020. Shoreface mesoscale morphodynamics: a review. Earth-Science Rev. 209 https://doi.org/10.1016/j.earscirev.2020.103330.

Hartman, M., Kennedy, A.B., 2016. Depth of closure over large regions using airborne bathymetric lidar. Mar. Geol. 379, 52–63. https://doi.org/10.1016/j.margeo.2016.05.012.

Hinton, C., Nicholls, R.J., 1998. Spatial and temporal behaviour of depth of closure along the Holland coast. Proc. Coast. Eng. Conf. 3, 2913–2925. https://doi.org/10.1061/9780784404119.221.

Horn, D.P., Walton, S.M., 2007. Spatial and temporal variations of sediment size on a mixed sand and gravel beach. Sediment. Geol. 202, 509–528. https://doi.org/10.1016/j.sedgeo.2007.03.023.

Jacobs, W., Le Hir, P., Van Kesteren, W., Cann, P., 2011. Erosion threshold of sand-mud mixtures. Cont. Shelf Res. 31, 14–25. https://doi.org/10.1016/j.csr.2010.05.012.

Kraus, N.C., Larson, M., Wise, R.A., 1998. Depth of closure in beach fill design. Coastal Engineering. Technical Note CETN II-40, 3/98.U.S. Army Engineer Waterways Experiment Station, Coastal and Hydraulics Laboratory, Proceedings of the 1999 National Conference on Beach Preservation Technology. Vicksburg, MS, p.13.

Krumbein, W.C., Pettijohn, F.J., 1938. Manual of Sedimentary Petrography. Appleton-Century-Crofts, New York.

McCarron, C.J., Van Landeghem, K.J.J., Baas, J.H., Amoudry, L.O., Malarkey, J., 2019. The hiding-exposure effect revisited: a method to calculate the mobility of bimodal sediment mixtures. Mar. Geol. 410, 22–31. https://doi.org/10.1016/j.margeo.2018.12.001.

Mitchener, H., Torfs, H., 1995. Erosion of mud sand mixtures. Coast. Eng. 29, 223.

National Network of Regional Coastal Monitoring Programmes., n.d. Pevensey Bay wave buoy statistics: average values for all years [WWW Document]. URL https://coastalmonitoring.org/realtimedata/?chart=77&tab=stats&disp_option=&data_type=table&year=All years (accessed 12.11.23).

New Forest District Council, 2020. Metadata for Hydrographic Survey 4cSU23_20200915.

Nicholls, R.J., Birkemeier, W.A., Hallermeier, R.J., 1996. Application of the depth of closure concept. Proc. Coast. Eng. Conf. 4, 3874–3887. https://doi.org/10.1061/9780784402429.299.

Nicholls, R.J., Birkemeier, W.A., Lee, G., 1998a. Evaluation of depth of closure using data from Duck, NC, USA. Mar. Geol. 148, 179–201.

Nicholls, R.J., Larson, M., Capobianco, M., Birkemeier, W.A., 1998b. Depth of closure: improving understanding and prediction. Proc. Coast. Eng. Conf. 3, 2888–2901. https://doi.org/10.1061/978078 4404119.219.

Ortiz, A.C., Ashton, A.D., 2016. Exploring shoreface dynamics and a mechanistic explanation for a morphodynamic depth of closure. Case Rep. Med. 121, 442–464. https://doi.org/10.1002/2015 JF003699.

Pagán, J.I., Villacampa, Y., Aragonés, L., López, I., 2017. A software application to obtain the depth of closure from beach profile data. Int. J. Comput. Methods Exp. Meas. 5, 750–759. https://doi.org/10.2495/CMEM-V5-N5-750-759.

Panagiotopoulos, I., Sylaios, G., Collins, M.B., 1994. Threshold studies of gravel size particles under the co-linear combined action of waves and currents. Sedimentology 41, 951–962. https://doi.org/10.1111/j.1365-3091.1994.tb01434.x.
Parkinson, R.W., Ogurcak, D.E., 2018. Beach nourishment is not a sustainable strategy to mitigate climate change. Estuar. Coast. Shelf Sci. 212, 203–209. https://doi.org/10.1016/j.ecss.2018.07.011.
Polska, L., Cerkowniak, G.R., Ostrowski, R., Stella, M., 2015. Bulletin of the Maritime Institute in Gdańsk Depth of Closure in the Multi-Bar Non-tidal Nearshore Zone of the Baltic Sea : Lubiatowo (Poland) Case Study Głębokość zamknięcia W Wielorewowej bezpływowej Strefie 180–188. https://doi.org/10.5604/12307424.1185577.
Robertson, V.W., Zhang, K., Finkl, C.W., Whitman, D., 2008. Hydrodynamic and geologic influence of event-dependent depth of closure along the South Florida Atlantic Coast. Mar. Geol. 252, 156–165. https://doi.org/10.1016/j.margeo.2008.03.018.
de Schipper, M.A., Ludka, B.C., Raubenheimer, B., Luijendijk, A.P., Schlacher, T.A., 2021. Beach nourishment has complex implications for the future of sandy shores. Nat. Rev. Earth Environ. 2, 70–84. https://doi.org/10.1038/s43017-020-00109-9.
Shoreline Surveys Ltd, 2021. J1877 - Data Collection Parameters.
Soulsby, R., 1997. Dynamics of Marine Sands. Thomas Telford, London.
Staudt, F., Gijsman, R., Ganal, C., Mielck, F., Wolbring, J., Hass, H.C., Goseberg, N., Schüttrumpf, H., Schlurmann, T., Schimmels, S., 2021. The sustainability of beach nourishments: a review of nourishment and environmental monitoring practice. J. Coast. Conserv. 25 https://doi.org/10.1007/s11852-021-00801-y.
Sutherland, J., Thomas, I., 2011. The management of Pevensey shingle barrier. Ocean Coast. Manag. 54, 919–929. https://doi.org/10.1016/j.ocecoaman.2011.07.004.
Taylor, J.A., Murdock, A.P., Pontee, N.I., 2004. A macroscale analysis of coastal steepening around the coast of England and Wales. Geogr. J. 170, 179–188. https://doi.org/10.1111/j.0016-7398.2004.00119.x.
Thomas, I., 2015. Long-term loss of beach material from the Eastern English Channel. Proc. Inst. Civ. Eng. Marit. Eng. 168, 174–181. https://doi.org/10.1680/jmaen.15.00025.
Townsend, D., Leyland, J., Kassem, H., Thompson, C., Townend, I., 2023. Linking nearshore morphological change to long term observed sand loss from a mixed sediment beach. In: Vienna (Ed.), EGU General Assembly. https://doi.org/10.5194/egusphere-egu23-8572.
Udo, K., Ranasinghe, R., Takeda, Y., 2020. An assessment of measured and computed depth of closure around Japan. Sci. Rep. 10, 1–8. https://doi.org/10.1038/s41598-020-59718-5.
USACE, 1984. Shore Protection Manual. Vicksburg, USA.
Valiente, N.G., Masselink, G., Scott, T., Conley, D., 2017. Depth of Closure along an Embayed, Macro-Tidal and Exposed Coast: A Multi-Criteria Approach. Coast, Dyn.
Valiente, N.G., Masselink, G., Scott, T., Conley, D., McCarroll, R.J., 2019. Role of waves and tides on depth of closure and potential for headland bypassing. Mar. Geol. 407, 60–75. https://doi.org/10.1016/j.margeo.2018. 10.009.
Watt, T., Dornbusch, U., Moses, C., Robinson, D., 2006. Surface sediment distribution patterns on mixed beaches in response to wave conditions. Coast. Dyn. 2005 - Proc. Fifth Coast. Dyn. Int. Conf., 40855 https://doi.org/10.1061/40855(214)17.
Weggel, J.R., 1972. Maximum Breaker Height. J. Waterw. Harb. Coast. Eng, Div, p. 98.